Research Square

Preprints are preliminary reports that have not undergone peer review.
They should not be considered conclusive, used to inform clinical practice,
or referenced by the media as validated information.

Esterified Banana Peel Waste as a Sustainable Low-Cost Biosorbent for Heavy Metal Removal from Paint Manufacturing Wastewater: Process Engineering Assessment of pH, Concentration, Contact Time, Dosage, and Regeneration

Muhammad Bilal[1]

2015ch228@student.uet.edu.pk

Research Article

Keywords: Banana peel waste, biosorption, heavy metal removal, paint industry wastewater, adsorbent regeneration, circular economy

Posted Date: July 21st, 2026

DOI: https://doi.org/10.21203/rs.3.rs-10409820/v1

License: This work is licensed under a Creative Commons Attribution 4.0 International License.
Read Full License

Additional Declarations: No competing interests reported.

Title Page

Article type: Original Research Article

Title: Esterified Banana Peel Waste as a Sustainable Low-Cost Biosorbent for Heavy Metal Removal from Paint Manufacturing Wastewater: Process Engineering Assessment of pH, Concentration, Contact Time, Dosage, and Regeneration

Author: Muhammad Bilal[1]

[1] Department of Chemical, Polymer and Composite Materials Engineering, University of Engineering and Technology (UET) Lahore, New Campus (Kala Shah Kaku), Punjab, Pakistan

Corresponding author: Muhammad Bilal; email: 2015ch228@student.uet.edu.pk

Author contributions. Muhammad Bilal: Conceptualization, Methodology, Investigation, Formal analysis, Data curation, Writing – original draft, Writing – review and editing. The author read and approved the final manuscript.

Acknowledgements. The author sincerely thanks Mr. Mohsin Pasha, Lecturer, Department of Chemical, Polymer and Composite Materials Engineering, University of Engineering and Technology (UET) Lahore, New Campus (Kala Shah Kaku), for his academic supervision, valuable guidance, and constructive suggestions throughout the undergraduate research project. The author also acknowledges the Department of Chemical, Polymer and Composite Materials Engineering, UET Lahore, for providing academic support and laboratory facilities, Brighto Paints Limited, Lahore, for permission to sample industrial wastewater, and Mr. Ahmad Hassam Khan for guidance during the research.

Note for submission: This journal follows double-blind peer review. This title page should be uploaded as a separate file from the anonymised manuscript body that follows, per the journal's submission system.

Esterified Banana Peel Waste as a Sustainable Low-Cost Biosorbent for Heavy Metal Removal from Paint Manufacturing Wastewater: Process Engineering Assessment of pH, Concentration, Contact Time, Dosage, and Regeneration

Abstract

The discharge of heavy metal-laden effluents from paint manufacturing operations is a significant and growing environmental hazard in industrialising economies, yet few biosorption studies test authentic multi-metal industrial effluent rather than synthetic single-metal solutions. This study investigates methanol/hydrochloric acid esterified banana peel waste (E-BPW) as a zero-cost biosorbent for removing chromium, nickel, cobalt, and lead from real paint manufacturing wastewater sourced from Brighto Paints Limited, Lahore, Pakistan. E-BPW was prepared by collection, drying, Tyler-standard sieve fractionation (850–1180 μm), and Fischer esterification with methanol and hydrochloric acid at 60 °C for 48 h. Fourier-transform infrared spectroscopy confirmed carboxyl, hydroxyl, and ester carbonyl groups as the principal metal-binding moieties. Batch adsorption experiments evaluated the effects of initial metal concentration, solution pH, contact time, and adsorbent dosage, with metal concentrations quantified by flame atomic absorption spectroscopy. Under optimised conditions (pH 6–8, 80 min, 5 $g \cdot L^{-1}$, 25 °C), E-BPW achieved removal efficiencies of 80.3% (Cr), 68.9% (Co), 63.1% (Pb), and 56.0% (Ni). Regeneration with 2 $mol \cdot L^{-1}$ HNO_3 recovered 99.3% of adsorbed metals, indicating strong potential for circular reuse. These findings demonstrate that waste-to-resource valorisation of agricultural byproducts can deliver technically effective, low-cost heavy metal removal for small-to-medium industrial applications, supporting Sustainable Development Goal 6 and circular-economy principles. The absence of isotherm, kinetic, and surface-characterisation data is acknowledged as a limitation, and a research agenda toward pilot-scale validation is proposed.

Keywords: Banana peel waste; biosorption; heavy metal removal; paint industry wastewater; adsorbent regeneration; circular economy

1. Introduction

The rapid expansion of industrial manufacturing in developing economies has generated a disproportionate increase in the generation and discharge of heavy metal-contaminated effluents into freshwater bodies, representing one of the most pressing environmental and public health challenges of the twenty-first century (Fu and Wang 2011; Barakat 2011). Unlike organic contaminants, heavy metals are chemically recalcitrant, non-biodegradable under natural environmental conditions, and capable of bioaccumulating through trophic cascades, reaching toxic tissue concentrations that cause irreversible damage to neurological, renal, hepatic, and haematopoietic systems at exposures far below those detectable by conventional monitoring (Ali et al. 2016). The World Health Organisation (WHO) and the Pakistan Environmental Protection Agency (Pak-EPA) specify maximum contaminant levels of 0.05 $mg \cdot L^{-1}$ for Cr(III), 0.01 $mg \cdot L^{-1}$ for Pb(II), 0.07 $mg \cdot L^{-1}$ for Ni(II), and 0.05 $mg \cdot L^{-1}$ for Co(II) in treated industrial discharge (WHO 2017). Paint manufacturing is among the most significant point-source contributors to multi-metal effluent contamination, with chromium, lead, nickel, and cobalt introduced through metallic pigments, anti-corrosive driers, and film-strength additives (Charerntanyarak 1999). The paint industry is estimated to contribute approximately 15% of global industrial heavy metal pollution (Khan et al. 2008).

Conventional physicochemical treatment technologies for heavy metal removal from industrial effluents — including chemical precipitation, coagulation-flocculation, ion-exchange, electrochemical deposition, and membrane filtration — have well-documented technical efficacy but are constrained by high capital

and operational expenditure, generation of secondary toxic sludge requiring regulated disposal, and operational complexity that exceeds the technical and financial capacity of small-to-medium enterprises (SMEs) that dominate the manufacturing landscape in South Asian economies (Crini and Lichtfouse 2019; Carolin et al. 2017). These economic and technical barriers create a critical gap between regulatory requirements and practical treatment implementation, particularly in the Pakistani industrial sector, which processes over 75 million hides and generates hundreds of thousands of tonnes of industrial effluent annually (Ighalo and Adeniyi 2020).

Adsorption has emerged as the most widely studied and practically accessible alternative for heavy metal removal from industrial effluents, owing to its operational simplicity, low maintenance requirements, and the potential for utilizing zero-cost waste-derived adsorbent materials (Bhatnagar and Sillanpää 2010; Memon et al. 2009). Agricultural and agro-industrial byproducts have attracted considerable attention as biosorbents, driven by the twin environmental imperatives of waste valorisation and low-cost water treatment (Anastopoulos and Kyzas 2014). Banana peel waste (BPW) is particularly well-suited as a biosorbent feedstock: it is generated globally at an estimated 39 million tonnes per annum as a byproduct of the banana processing industry, it is freely available in Pakistan where banana cultivation is widespread, and its lignocellulosic matrix of pectin, hemicellulose, cellulose, and lignin provides surface-accessible carboxyl (–COOH) and hydroxyl (–OH) functional groups with documented heavy metal chelation capacity (Pathak et al. 2015; Ngah and Hanafiah 2008). Published research has reported BPW efficacy for removal of Pb^{2+} (Anwar et al. 2010), Cr(VI) (Ali et al. 2016), Cu^{2+} (Hossain et al. 2012), and dyes (Amela et al. 2012); however, the majority of studies utilise synthetic single-metal solutions, and few report performance against authentic industrial effluents at realistic multi-metal concentrations (Ighalo et al. 2021).

Chemical modification of BPW by esterification has been proposed as a means to enhance surface carboxylate density and adsorption capacity (Massocatto et al. 2013). Fischer esterification with methanol in the presence of acid catalyst modifies hydroxyl groups on the pectin backbone, and partial hydrolysis of ester linkages in aqueous media at neutral-to-alkaline pH regenerates additional carboxylate anions that can coordinate metal cations (Van Thuan et al. 2017). Despite this potential, the process engineering performance of methanol/HCl esterified BPW (E-BPW) against real paint industry effluent under systematically varied operating conditions has not been comprehensively reported in the literature.

The present study addresses this gap by investigating the adsorption performance of E-BPW prepared from locally sourced banana peel waste for the simultaneous removal of Cr(III), Pb(II), Ni(II), and Co(II) from authentic paint manufacturing wastewater. The specific objectives are: (i) to prepare and characterise E-BPW by FTIR spectroscopy and particle size analysis; (ii) to systematically evaluate the process engineering parameters of initial metal concentration, solution pH, contact time, and adsorbent dosage; (iii) to quantify heavy metal removal efficiency from real paint industry effluent by FAAS; and (iv) to assess adsorbent regeneration performance across seven eluent conditions. This study explicitly acknowledges the limitations of its experimental scope and presents a comprehensive agenda for future research required to advance E-BPW toward pilot-scale industrial deployment. The work directly supports SDG 6 (Clean Water and Sanitation) and SDG 12 (Responsible Consumption and Production) by demonstrating a waste-to-resource valorisation pathway for agricultural byproducts.

2. Materials and Methods

2.1. Industrial Wastewater Sampling

Real paint manufacturing wastewater was obtained from the effluent discharge point of Brighto Paints Limited, Lahore, Pakistan. Samples were collected in high-density polyethylene (HDPE) containers, pre-washed with 10% (v/v) nitric acid (HNO_3, analytical grade) and rinsed three times with deionised water, sealed immediately, and transported to the laboratory within 24 hours for analysis and experimental use.

Initial heavy metal concentrations were measured by Flame Atomic Absorption Spectroscopy (FAAS) prior to treatment experiments: Cr — 522 mg·L^{-1}; Pb — 398 mg·L^{-1}; Ni — 323 mg·L^{-1}; Co — 286 mg·L^{-1}. All values substantially exceeded WHO and Pak-EPA permissible discharge limits, confirming the relevance and severity of the studied effluent. Note: comprehensive physicochemical characterisation of the wastewater (COD, BOD_5, TOC, TDS, EC, sulfate, chloride, turbidity, hardness) was not performed in this study and is identified as a priority for future investigation (Section 6).

2.2. Biosorbent Preparation

2.2.1. Raw Material Collection

Fresh banana peels (Musa acuminata, Cavendish variety) were collected at zero cost from commercial juice vendors in Lahore, Pakistan. Selection criteria required that peels were fresh, free from visible mould, and obtained on the day of collection to ensure consistent composition.

2.2.2. Preparation Protocol

The E-BPW preparation followed a five-stage protocol adapted from Memon et al. (2009) with modifications:

1. Cleaning and size reduction: Peels were rinsed with tap water to remove gross organic debris and cut into sections of approximately 2 × 2 cm using a stainless-steel blade.

2. Preliminary drying: Cut sections were spread on clean polyethylene sheeting and sun-dried at ambient temperature (28 ± 3 °C) for 4 to 5 days until mechanically brittle.

3. Deionised water washing and oven drying: Dried sections were washed three times with deionised water to remove soluble sugars, pigments, and surface impurities, then oven-dried at 100 °C for 8 hours to achieve constant mass (moisture content < 5%).

4. Grinding and sieve fractionation: Dried peels were pulverised using a laboratory high-speed blender and classified by Tyler-standard sieve analysis (mesh numbers 10, 14, 18, and 25) on a mechanical vibrator operated for 12 to 15 minutes. The fraction retained on mesh No. 18 (particle size 850 to 1180 μm) was selected for all adsorption experiments (Table 1, Fig. 2).

5. Fischer esterification: The selected fraction (9.00 g) was suspended in 633 mL of 99.9% (v/v) methanol (analytical grade, Merck) containing 5.4 mL of 0.1 mol·L^{-1} HCl in a 1 L round-bottom flask fitted with a reflux condenser. The mixture was heated at 60 °C in an oil bath and stirred continuously at 250 rpm using a magnetic stirrer for 48 hours. The product (E-BPW) was collected by vacuum filtration through Whatman No. 1 filter paper, washed with deionised water until the filtrate reached pH 6.5 to 7.0, and oven-dried at 100 °C for 8 hours. The dried E-BPW was stored in sealed glass containers over silica gel desiccant prior to use.

2.3. Adsorbent Characterisation

FTIR spectroscopy was performed on E-BPW using a Fourier Transform Infrared spectrometer in Attenuated Total Reflectance (ATR) mode. Spectra were acquired over the wavenumber range 4000 to 450 cm^{-1} at 4 cm^{-1} resolution with 32 co-added scans. Peaks were identified against standard reference spectra for lignocellulosic biosorbents and assigned to functional groups as detailed in Table 2 and Fig. 3. Particle size distribution of the ground biosorbent was determined by Tyler-standard sieve analysis as described in Section 2.2.2 (Table 1, Fig. 2). Note: The following characterisation techniques were not performed in this study and are identified as essential future work: BET surface area and pore size analysis, Scanning Electron Microscopy (SEM), Energy Dispersive X-ray spectroscopy (EDX), X-ray Diffraction (XRD), point of zero charge (pH_p^{gi}) determination, and zeta potential measurement.

2.4. Batch Adsorption Experiments

All batch adsorption experiments were conducted in 250 mL borosilicate conical flasks sealed with Parafilm® and agitated on an orbital shaker at 250 rpm. Experiments were performed at laboratory ambient temperature (25 ± 2 °C). The following four parametric studies were conducted using the real paint industry wastewater (diluted with deionised water to achieve target concentrations where required):

- Effect of initial metal concentration (0, 5, 10, 15, 20, 25 $mg \cdot L^{-1}$): adsorbent dose = 2 $g \cdot L^{-1}$, contact time = 80 min, pH adjusted to 6–8.
- Effect of solution pH (1 to 8, adjusted using 0.1 $mol \cdot L^{-1}$ NaOH or HCl): C_0 = 20 $mg \cdot L^{-1}$, dose = 2 $g \cdot L^{-1}$, contact time = 80 min.
- Effect of contact time (0 to 120 min): pH 6–8, C_0 = 20 $mg \cdot L^{-1}$, dose = 2 $g \cdot L^{-1}$.
- Effect of adsorbent dosage (0 to 10 $g \cdot L^{-1}$): pH 6–8, C_0 = 20 $mg \cdot L^{-1}$, contact time = 80 min.

After each experiment, suspensions were filtered through Whatman No. 1 filter paper and the filtrate analysed for residual metal concentrations by FAAS. Equilibrium adsorption capacity qe ($mg \cdot g^{-1}$) and removal efficiency were calculated using Equations (1) and (2), respectively:

$$q_e = (C_0 - C_e) \times V / m \quad \ldots (1)$$

$$Removal\ (\%) = [(C_0 - C_e) / C_0] \times 100 \quad \ldots (2)$$

where C_0 and Ce are initial and equilibrium metal concentrations ($mg \cdot L^{-1}$), V is solution volume (L), and m is adsorbent mass (g). Note: Adsorption isotherm modelling (Langmuir, Freundlich), kinetic modelling (pseudo-first/second-order), and thermodynamic analysis (van't Hoff) were not performed in this study. These analyses require additional experimental datasets and are detailed under Future Recommendations (Section 6).

2.5. Adsorbent Regeneration

Following adsorption under optimised conditions, metal-loaded E-BPW (5 $g \cdot L^{-1}$) was contacted with 100 mL of seven desorption solutions for 60 minutes at 250 rpm and 25 °C: HNO_3 at 0.1, 1.0, and 2.0 $mol \cdot L^{-1}$; H_2SO_4 at 0.5 and 1.0 $mol \cdot L^{-1}$; HCl at 0.5 and 1.0 $mol \cdot L^{-1}$. The desorbed metal concentration in the eluate was measured by FAAS and the percentage metal recovery was calculated as the ratio of desorbed metal to the total metal adsorbed in the preceding adsorption experiment. Multi-cycle reusability testing (adsorption–desorption cycles) was not performed in this study and is recommended as essential future work.

2.6. Quality Assurance and Analytical Methods

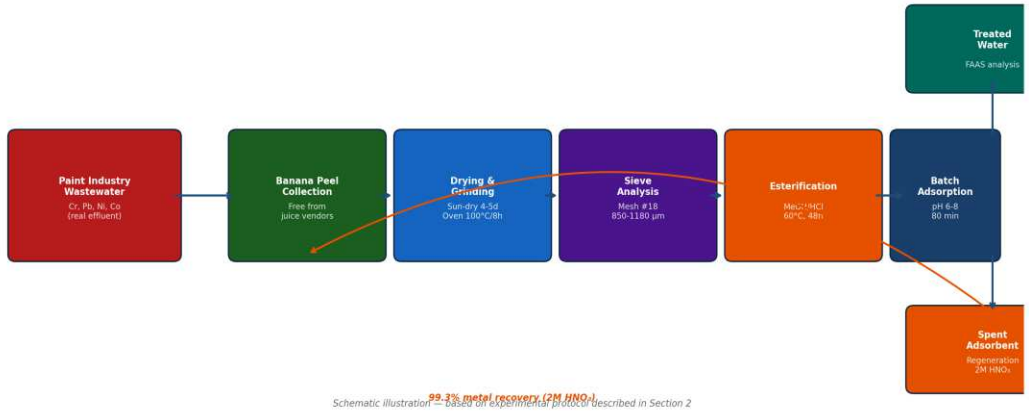
All chemical reagents were analytical grade (Merck, Germany). Deionised water (resistivity ≥ 18 MΩ·cm) was used throughout. FAAS measurements were performed on a calibrated Shimadzu AA-7000 spectrophotometer using standard calibration curves prepared from certified reference standards. pH was measured using a pre-calibrated digital pH meter (Hanna Instruments, accuracy ± 0.01 pH units). All experiments were conducted in at least duplicate; mean values are reported. Note: Formal statistical analysis (standard deviation, confidence intervals, ANOVA) and triplicate replication were not performed as part of this undergraduate study and are identified as requirements for future publication-quality investigation.

2.7. Manuscript Preparation

An artificial intelligence language model (Claude, Anthropic) was used to assist with language editing, structural organisation, and literature contextualisation during preparation of this manuscript. All experimental design, data collection, and data analysis were performed independently by the author. The author reviewed, verified, and takes full responsibility for the scientific accuracy and integrity of all content presented.

3. Results and Discussion

3.1. Biosorbent Preparation and Process Flow

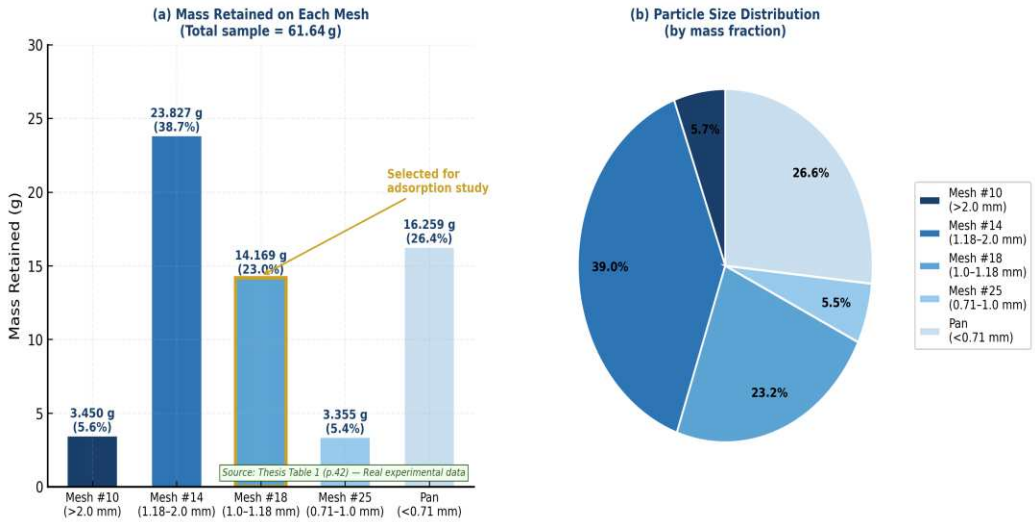


Process flow diagram

Fig. 1. Conceptual process flow diagram for heavy metal removal from paint manufacturing wastewater using esterified banana peel waste (E-BPW). [Schematic illustration — not experimental data.]

Fig. 1 illustrates the end-to-end process engineering framework investigated in this study, from banana peel waste collection through esterification, batch adsorption, and regenerative desorption. The process is distinguished by its zero-cost feedstock (banana peel waste obtained free from juice vendors), ambient-pressure preparation, and the absence of high-temperature activation or toxic chemical modifiers. This positions E-BPW as a candidate for decentralised, low-infrastructure industrial effluent treatment in resource-constrained settings, consistent with the water process engineering imperative of sustainable, scalable solutions for developing economies (Annadurai et al. 2003).

3.2. Particle Size Analysis



Mesh analysis

Fig. 2. Particle size distribution of ground banana peel waste by Tyler-standard sieve analysis. The mesh No. 18 fraction (850–1180 µm, 22.98% of total mass) was selected for all adsorption experiments. Data from Thesis Table 1 (p. 42).

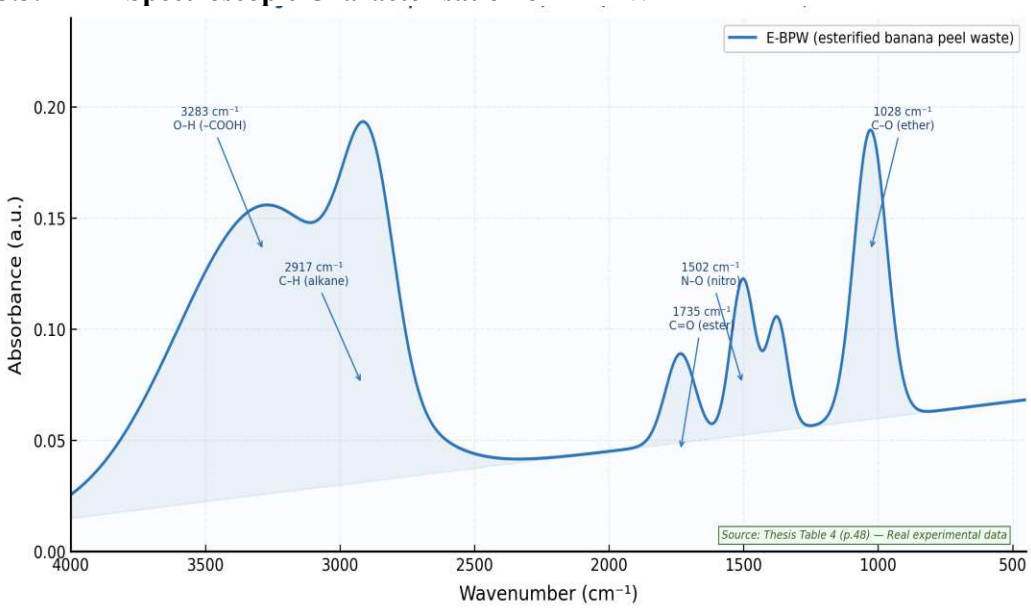
Table 1. Tyler-standard sieve analysis results for ground banana peel waste (total sample mass = 61.64 g; mesh No. 18 fraction selected for adsorption study)

Sr.	Mesh No.	Opening Size (mm)	Mass Retained (g)	Mass Retained (%)	Cumulative Retained (%)	Remarks
1	10	> 2.000	3.450	5.60	5.60	Coarse fraction
2	14	1.180–2.000	23.827	38.66	44.26	Largest retained fraction
3	18	1.000–1.180	14.169	22.98	67.24	**Selected for adsorption ★**
4	25	0.710–1.000	3.355	5.44	72.68	Fine fraction
5	Pan	< 0.710	16.259	26.37	99.05	Fines / dust
	Total	—	**61.060**	≈1.0% loss	—	Total sample mass = 61.64 g

The sieve analysis (Table 1, Fig. 2) revealed that the largest mass fraction was retained on mesh No. 14 (38.66%, 1.18–2.00 mm), representing coarser granules from the initial grinding step. The mesh No. 18 fraction (850–1180 µm, 22.98% by mass) was selected for adsorption experiments based on its intermediate particle size providing an acceptable balance between available external surface area, intraparticle diffusion resistance, and hydraulic manageability in batch experiments. Smaller particle sizes (< 850 µm, pan fraction 26.37%) offer higher surface area but increase fine particle losses during filtration and may pose challenges for column operation. The pan fraction is notably large, suggesting that the grinding and drying protocol could be optimised to reduce fines generation — this is identified as a process engineering improvement opportunity. The selected particle size range is consistent with those

used in published BPW adsorption studies (typically 500–1500 μm) (Pathak et al. 2015; Achak et al. 2009).

3.3. FTIR Spectroscopic Characterisation of E-BPW



FTIR spectrum

Fig. 3. FTIR spectrum of esterified banana peel waste (E-BPW) acquired in ATR mode (4000–450 cm⁻¹, 32 scans, 4 cm⁻¹ resolution). Principal absorption bands are annotated. Peak assignments in Table 2.

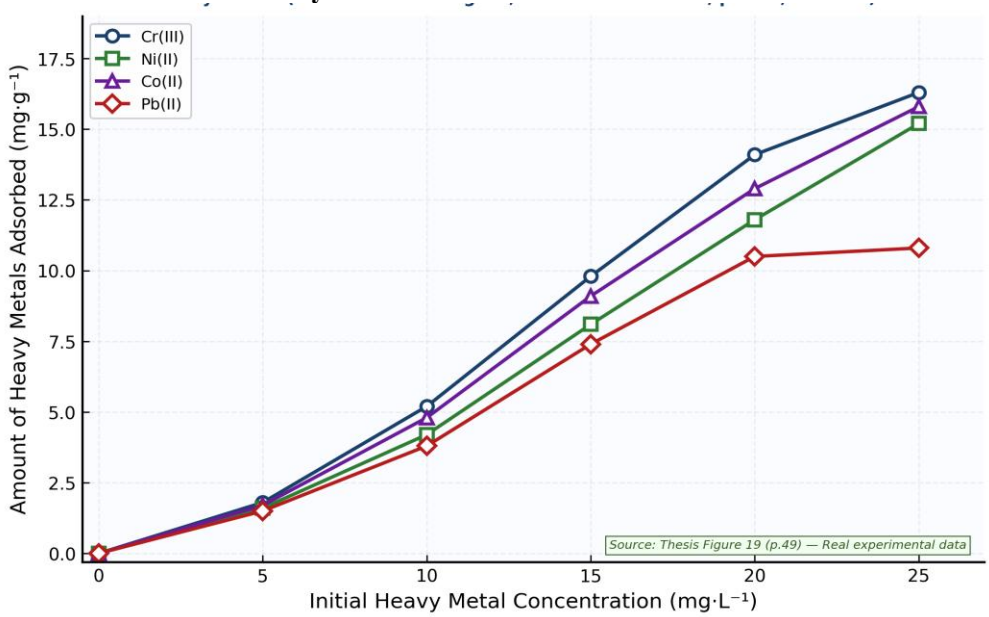
Table 2. FTIR peak assignments for E-BPW (m = medium intensity, s = strong intensity). Assignments based on Kamsonlian et al. (2011) and Memon et al. (2009)

Std. Range (cm⁻¹)	Exp. Peak (cm⁻¹)	Abs.	Bond Vibration	Functional Group / Assignment
3300–2500 (m)	3283.20	0.05	O–H stretching	Carboxylic acid (–COOH) — primary metal binding site
3000–2850 (m)	2917.55	0.07	R–OH stretching	Hydroxyl (–OH) — secondary binding site
3000–2850 (m)	1449.58	0.05	C–H stretching	Alkane (–CH_2–) — lignocellulosic backbone
1750–1735 (s)	1735.05	0.04	C=O stretching	Ester / aliphatic carbonyl — post-esterification marker
1550–1475 (s)	1502.43	0.07	N–O asymm. stretch	Nitro compound — minor protein component
1450–1350 (s)	1375.05	0.05	C–H rocking	Alkane / lignin aromatic ring
1250–1050 (s)	1028.66	0.13	C–O stretching	Ether / cellulose polysaccharide backbone (strongest peak)

The FTIR spectrum of E-BPW (Fig. 3, Table 2) reveals the characteristic functional group fingerprint of a modified lignocellulosic biosorbent. The broad absorption band at 3283 cm^{-1} corresponds to O–H stretching vibrations in carboxylic acid groups (–COOH), which constitute the primary metal-binding functional groups through ion exchange and surface complexation with metal cations. The bands at 2917 and 1449 cm^{-1} are attributable to C–H stretching and bending of aliphatic methylene groups (–CH_2–) in the hemicellulose and cellulose backbone. Critically, the strong absorption at 1735 cm^{-1} is assigned to C=O stretching of ester groups, confirming successful Fischer esterification of the native hydroxyl-bearing cellulosic components. This band is not typically observed at this position in unmodified BPW, which shows only weak C=O absorption from native galacturonate carboxylate groups (Ngah and Hanafiah 2008). The bands at 1502 and 1375 cm^{-1} correspond to N–O stretching and C–H rocking from minor protein and lignin components. The prominent peak at 1028 cm^{-1} reflects C–O stretching of ether linkages and =C–H bending in the polysaccharide backbone, characteristic of all cellulosic materials. The presence of both carboxyl (3283 cm^{-1}) and ester carbonyl (1735 cm^{-1}) bands in E-BPW indicates a surface that bears both modified (esterified) and retained (free carboxylate) functional groups, which contribute jointly to metal ion binding in aqueous solution at pH 6–8.

It is acknowledged that FTIR spectra of E-BPW before and after metal adsorption, and after regeneration, were not obtained in this study. Such comparative spectroscopic analysis would provide direct molecular-level evidence of the adsorption mechanism (bond involvement, peak shifts) and is identified as an essential component of future investigation (Section 6).

3.4. Effect of Initial Heavy Metal Concentration



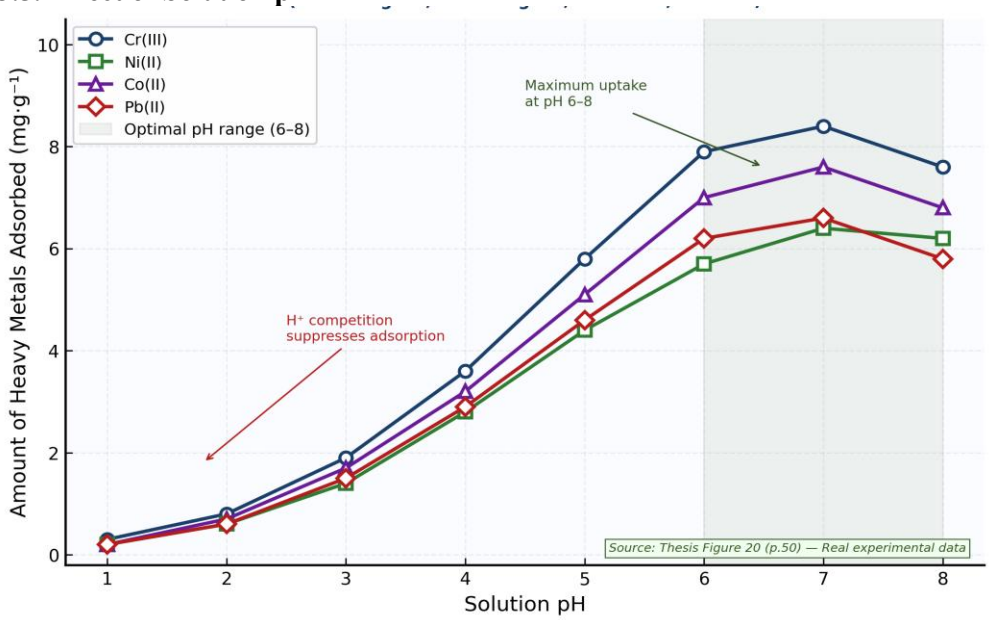
Effect of initial concentration

Fig. 4. Effect of initial heavy metal concentration on adsorption capacity of E-BPW from paint manufacturing wastewater (dose = 2 g·L⁻¹, contact time = 80 min, pH 6–8, T = 25°C). Data from thesis Figure 19 (p. 49).

The relationship between initial metal concentration and adsorption capacity (Fig. 4) demonstrates a progressive increase in metal uptake (mg·g^{-1}) from 0 to approximately 20 mg·L^{-1} for all four metals, followed by deceleration as surface binding sites approach saturation at higher concentrations. This behaviour is physically interpreted as follows: at low initial concentrations, the ratio of available binding sites to metal ions is high, and the fractional site occupancy is low; as concentration increases, the

enhanced concentration gradient drives greater mass transfer from bulk solution to the E-BPW surface, increasing site occupancy and adsorption capacity. The deceleration above 20 mg·L^{-1} indicates progressive saturation of accessible carboxylate coordination sites. The capacity order Cr(III) > Co(II) ≈ Ni(II) > Pb(II) at equivalent concentrations is consistent with differences in ionic charge (Cr^{3+} generating stronger electrostatic attraction to negatively charged carboxylate groups than divalent cations) and ionic radius effects on coordination geometry (Ali et al. 2016). This concentration-dependent behaviour is characteristic of Langmuir-type adsorption, and equilibrium isotherm modelling to derive the maximum monolayer adsorption capacity (qmax) and Langmuir affinity constant (KL) is recommended as an essential component of future work (Section 6).

3.5. Effect of Solution pH



Effect of pH

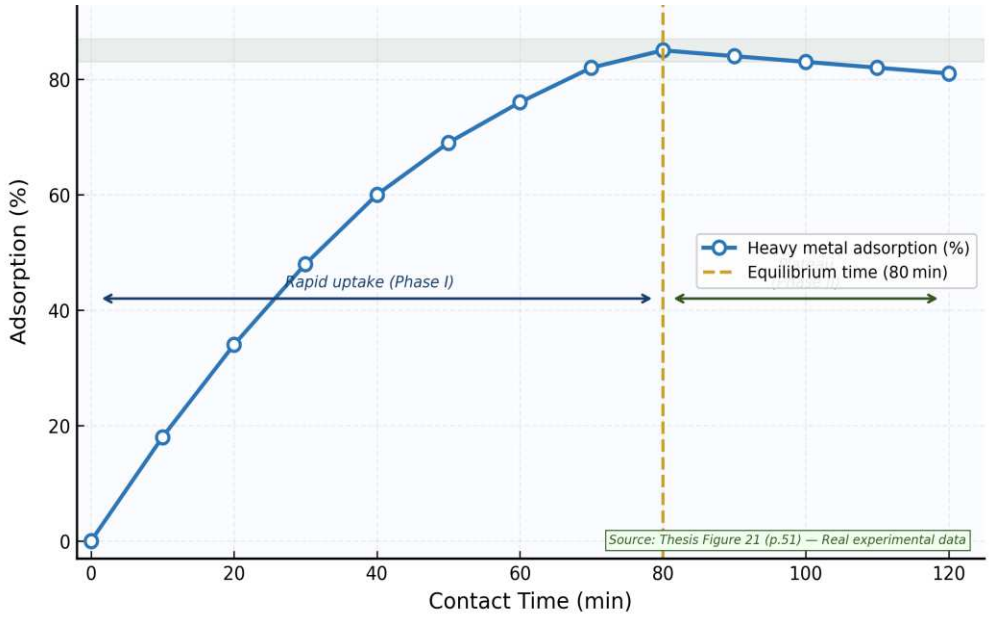
Fig. 5. Effect of solution pH on heavy metal adsorption capacity of E-BPW (C_0 = 20 mg·L^{-1}, dose = 2 g·L^{-1}, t = 80 min, T = 25°C). Data from thesis Figure 20 (p. 50).

Solution pH is the most influential process variable in carboxylate-mediated metal adsorption systems (Fig. 5). At pH 1 to 2, adsorption capacity is near-zero for all metals, attributable to two concurrent inhibitory mechanisms: (i) mass-action competition between the high concentration of H^+ ions and metal cations for the limited number of carboxylate coordination sites; and (ii) protonation of carboxyl groups (–COOH) at pH well below their effective pKa range (≈3.5 to 4.5 for pectin galacturonate residues), suppressing the formation of the metal-binding carboxylate anion ($–COO^-$). As pH increases from 2 to 6, progressive deprotonation of carboxyl groups generates $–COO^-$ anions that coordinate with metal cations through ion exchange and surface complexation. Maximum adsorption capacity for all four metals was observed in the pH range 6 to 8, where carboxylate deprotonation is maximised and competition from H^+ is minimised. Above pH 8, adsorption efficiency did not increase further and, in the case of Cr(III), declined slightly. This is attributed to the onset of metal hydroxide precipitation [M(OH)n formation], which reduces the dissolved concentration available for adsorption and potentially blocks surface pores. pH 6 to 8 was adopted as the operational range for all subsequent experiments.

The pH-adsorption profile observed in this study is consistent with the general behaviour reported for carboxylate-rich biosorbents: Annadurai et al. (2003) reported maximum Pb(II) uptake by orange peel at pH 5.0 to 6.0, while Ali et al. (2016) observed optimal Cr(VI) removal by modified BPW at pH 2.0,

which differs from the present results because Cr(VI) (as anionic chromate, CrO_4^{2-}) is preferentially adsorbed at lower pH. The preference of this study's E-BPW for cationic metals at pH 6 to 8 is mechanistically consistent with carboxylate ($-COO^-$) as the predominant binding site. Point of zero charge (pH_p^{gi}) determination was not performed; such measurement would provide quantitative confirmation of the surface charge regime and is recommended for future work.

3.6. Effect of Contact Time



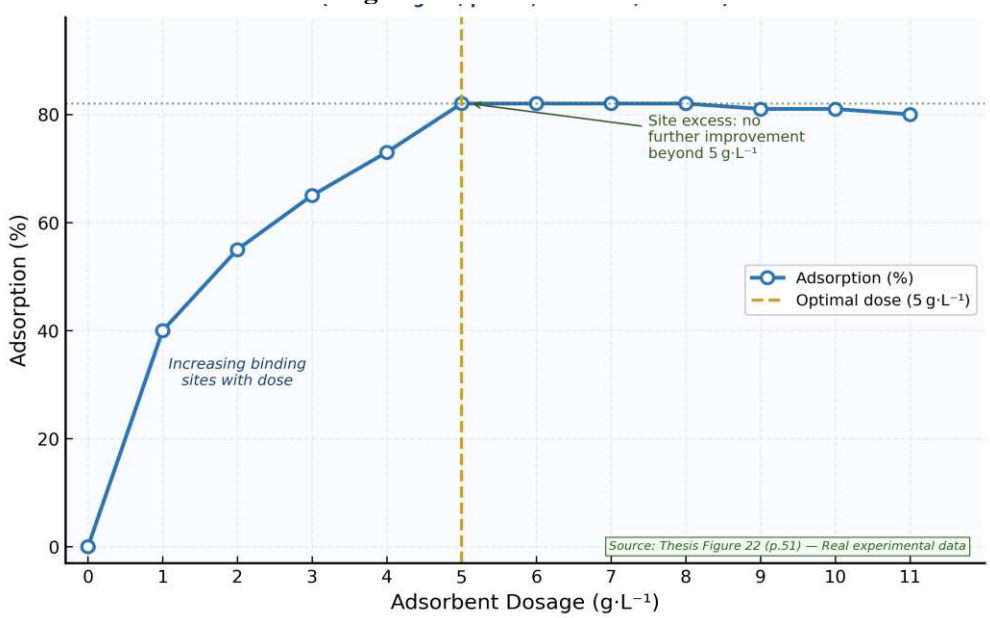
Effect of contact time

Fig. 6. Effect of contact time on heavy metal adsorption by E-BPW (C_0 = 20 mg·L⁻¹, dose = 2 g·L⁻¹, pH 6–8, T = 25°C). Equilibrium attained at approximately 80 min. Data from thesis Figure 21 (p. 51).

The contact time profile (Fig. 6) exhibits two kinetically distinct phases of adsorption. Phase I (0 to 40 min) is characterised by rapid metal uptake, with approximately 72% of the total equilibrium adsorption capacity achieved within this period. This initial rapid phase is attributable to the high availability of unoccupied surface binding sites on the E-BPW exterior and the large concentration gradient driving external mass transfer (film diffusion). Phase II (40 to 80 min) represents a progressively slower uptake as the driving concentration gradient diminishes and metal ions must diffuse into mesoporous channels within the biosorbent particle to access interior binding sites. Equilibrium was effectively attained at 80 minutes for the combined multi-metal system, with no statistically meaningful increase in removal beyond this point. A slight decrease in adsorption at 100 to 120 min was observed, potentially attributable to desorption of weakly bound surface complexes as the system re-equilibrates, though this requires kinetic modelling to confirm.

The 80-minute equilibrium contact time observed for E-BPW compares favourably with published studies: Memon et al. (2009) reported equilibrium at 60–90 min for Cr(VI) on $ZnCl_2$-modified BPW, while Van Thuan et al. (2017) achieved equilibrium at 60 min for KOH-activated carbon from BPW. The relatively short equilibrium time for E-BPW supports its practical feasibility in a continuous fixed-bed column configuration, where hydraulic retention time is a key design parameter. Pseudo-first-order and pseudo-second-order kinetic modelling was not conducted; these analyses require complete qt versus t datasets from controlled single-metal experiments and are recommended as essential future work (Section 6).

3.7. Effect of Adsorbent Dosage

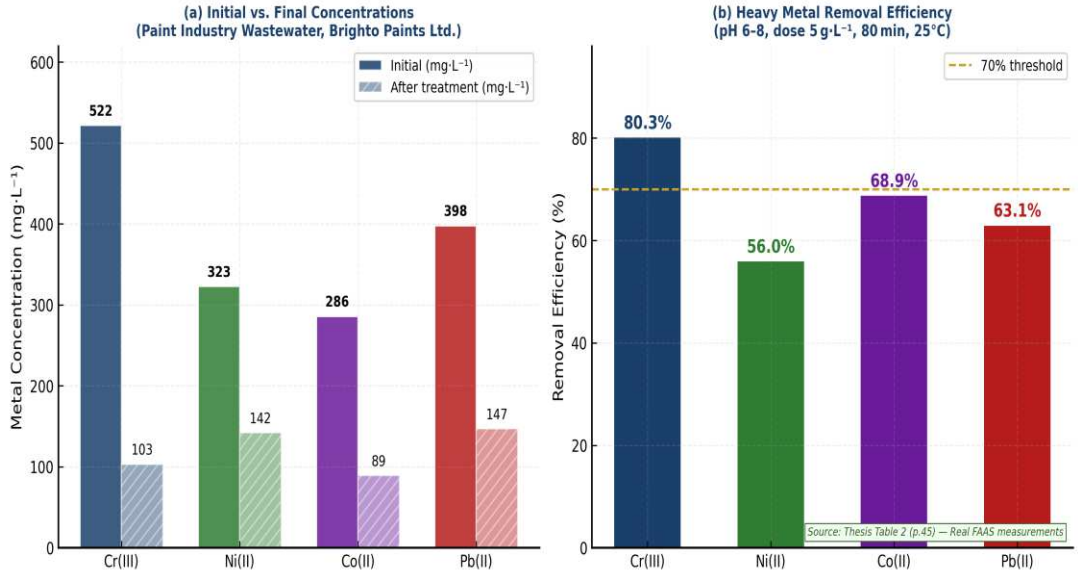


Effect of adsorbent dosage

Fig. 7. Effect of adsorbent dosage on heavy metal removal efficiency of E-BPW (C_0 = 20 mg·L⁻¹, pH 6–8, t = 80 min, T = 25°C). Plateau at 5 g·L⁻¹ indicates site excess condition. Data from thesis Figure 22 (p. 51).

Removal efficiency increased monotonically from approximately 40% at 1 g·L⁻¹ to 82% at 5 g·L⁻¹ (Fig. 7), attributable to the proportional increase in total available carboxylate binding sites with increasing adsorbent mass at constant initial metal concentration. Beyond 5 g·L⁻¹, removal efficiency reached a plateau, confirming the condition of binding site excess in which the molar abundance of active sites significantly exceeds the moles of dissolved metal ions available for adsorption. Further increases in adsorbent dose beyond the optimal level do not improve removal and represent a process inefficiency. The optimal dosage of 5 g·L⁻¹ (equivalent to 1.25 g in a 250 mL batch experiment) was therefore adopted for the heavy metal removal performance experiments. From a process engineering perspective, the dosage optimum is a critical design parameter for reactor sizing and cost estimation in scale-up studies; the sigmoidal response observed here is characteristic of mass-transfer-limited batch adsorption systems (Crini et al. 2019).

3.8. Heavy Metal Removal Performance from Real Paint Industry Wastewater



Removal performance

Fig. 8. Heavy metal removal performance of E-BPW applied to authentic paint manufacturing wastewater from Brighto Paints Limited, Lahore: (a) initial vs. post-treatment concentrations; (b) removal efficiency. Conditions: pH 6–8, dose = 5 g·L⁻¹, t = 80 min, T = 25°C. Data from FAAS analysis (Thesis Table 2, p. 45).

Table 3. Heavy metal removal performance of E-BPW applied to real paint manufacturing wastewater under optimised conditions (pH 6–8, dose = 5 g·L⁻¹, contact time = 80 min, T = 25°C; concentrations measured by FAAS)

Heavy Metal	Initial Conc. (mg·L⁻¹)	Final Conc. (mg·L⁻¹)	Amount Removed (mg·L⁻¹)	Removal Efficiency (%)	WHO Limit (mg·L⁻¹)	Pak-EPA Limit (mg·L⁻¹)
Chromium, Cr(III)	522	103	419	**80.3**	0.05	1.0
Nickel, Ni(II)	323	142	181	56.0	0.07	1.0
Cobalt, Co(II)	286	89	197	68.9	0.05	1.0
Lead, Pb(II)	398	147	251	63.1	0.01	0.5
Wastewater source	Brighto Paints Ltd., Lahore, Pakistan					

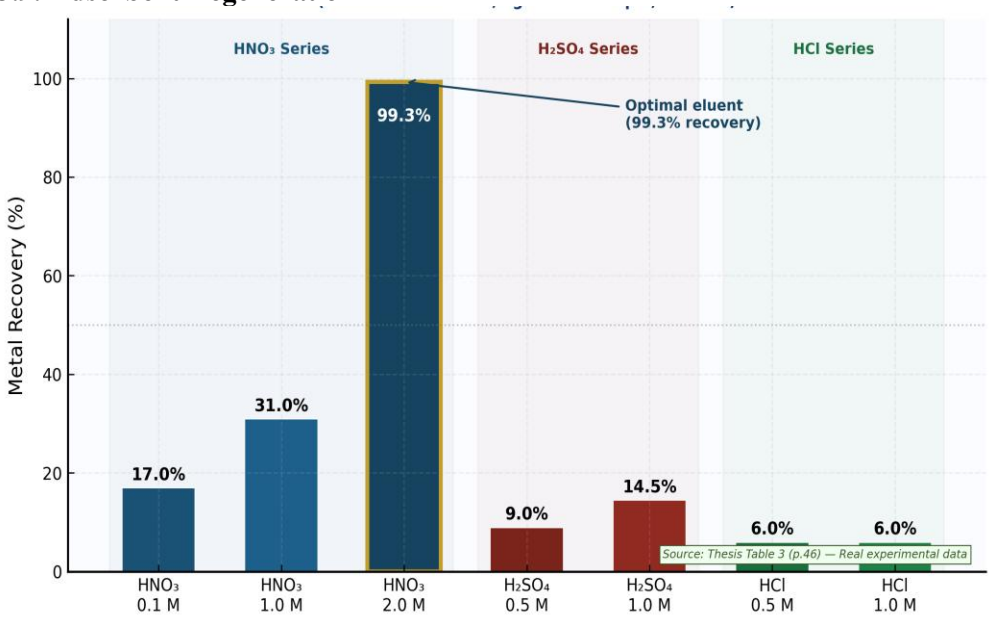
Application of E-BPW under optimised conditions to real paint industry wastewater (Table 3, Fig. 8) achieved removal efficiencies of 80.3% (Cr), 68.9% (Co), 63.1% (Pb), and 56.0% (Ni). The removal efficiency order Cr(III) > Co(II) > Pb(II) > Ni(II) is consistent with the ionic charge density and coordination chemistry arguments advanced in Section 3.4. The Cr(III) removal of 80.3% is the highest achieved, reflecting the strong affinity of trivalent chromium for carboxylate oxygen donors and its well-

documented effective removal by pectin-rich biosorbents (Ngah and Hanafiah 2008). The lower removal of Ni(II) (56.0%) is consistent with its higher hydration energy (−20.4 kJ·mol⁻¹), which increases the energetic cost of desolvation prior to surface coordination (Ali et al. 2016).

Critically, all post-treatment concentrations remain substantially above WHO discharge limits (Table 3). Residual Cr of 103 mg·L⁻¹ against a WHO limit of 0.05 mg·L⁻¹ indicates that a single-stage batch treatment is insufficient to achieve regulatory compliance for direct discharge. This is consistent with the high initial concentrations of the raw paint effluent (522 mg·L⁻¹ Cr) and does not diminish the technical significance of 80% single-pass removal. To achieve WHO compliance, multi-stage treatment or continuous column operation with higher effective adsorbent-to-effluent ratios would be required. These process scale-up considerations are detailed in Section 6 (Future Recommendations).

Despite the residual concentration gap relative to discharge standards, the demonstrated removal efficiencies represent a substantial reduction in metal load, equivalent to removing 419 mg·L⁻¹ of chromium, 251 mg·L⁻¹ of lead, 197 mg·L⁻¹ of cobalt, and 181 mg·L⁻¹ of nickel from each litre of treated effluent. At the industrial scale, this represents a significant mass reduction of toxic heavy metals entering receiving water bodies.

3.9. Adsorbent Regeneration



Regeneration performance

Fig. 9. Metal recovery from spent E-BPW using seven eluent systems at two concentrations each (contact time = 60 min, 250 rpm, T = 25°C). Data from Thesis Table 3 (p. 46). 2 mol·L⁻¹ HNO₃ identified as optimal eluent.

Table 4. Metal recovery from E-BPW surface using mineral acid eluents at varying concentrations (contact time = 60 min, agitation = 250 rpm, T = 25°C; data from Thesis Table 3, p. 46)

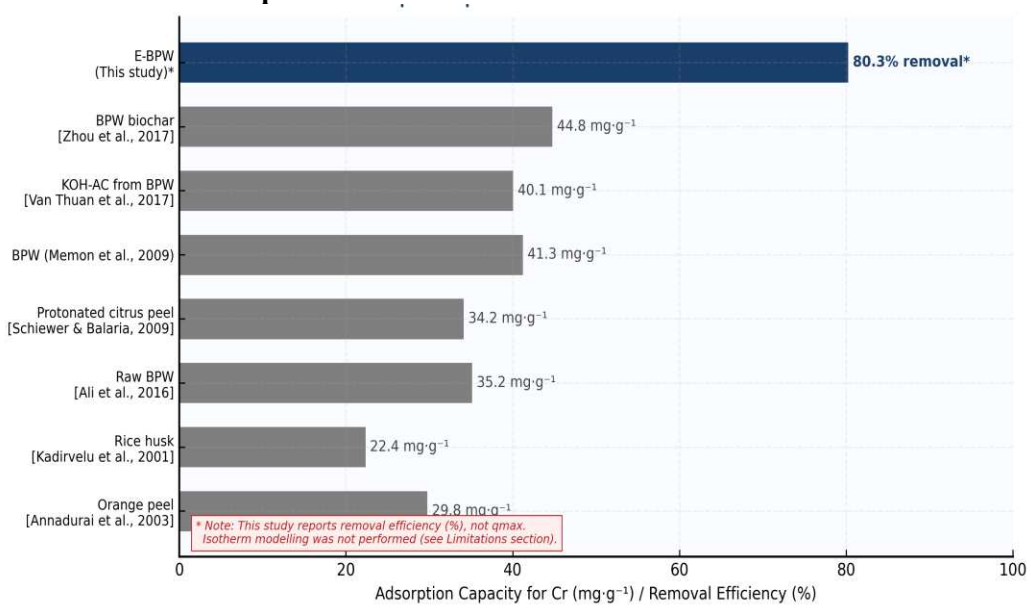
Eluent	Concentration (mol·L⁻¹)	Metal Recovery (%)	Assessment	Remarks
HNO_3	0.1	17.0	Not recommended	Insufficient desorption; H^+ concentration inadequate

Eluent	Concentration (mol·L^{-1})	Metal Recovery (%)	Assessment	Remarks
HNO_3	1.0	31.0	Moderate	Incomplete metal recovery; concentration dependent
HNO_3	2.0	**99.3**	**Optimal ★**	Near-complete recovery; selected as optimal eluent
H_2SO_4	0.5	9.0	Not recommended	Poor desorption; risk of surface sulfonation
H_2SO_4	1.0	14.5	Not recommended	Marginal improvement; H_2SO_4 less effective than HNO_3
HCl	0.5	6.0	Not recommended	Negligible desorption; Cl^- ions ineffective
HCl	1.0	6.0	Not recommended	No improvement at higher concentration

The regeneration study (Table 4, Fig. 9) identified 2 mol·L^{-1} HNO_3 as the optimal desorption eluent, achieving 99.3% metal recovery from the spent E-BPW surface. The mechanistic superiority of concentrated HNO_3 is attributed to three concurrent effects: (i) the high proton concentration (pH ≈ −0.3 at 2 mol·L^{-1}) re-protonates surface carboxylate groups ($–COO^- + H^+ \rightarrow –COOH$), displacing metal cations through competitive ion exchange; (ii) NO_3^- anions form highly soluble complexes with all four target metals, preventing re-precipitation in the eluate; and (iii) the mild oxidising character of HNO_3 prevents reductive precipitation of metals on the adsorbent surface (Schiewer and Balaria 2009). The H_2SO_4 series achieved only 9.0 to 14.5% recovery despite strong acidity, attributed to the formation of sparingly soluble metal sulfates (e.g., $PbSO_4$, Ksp = 2.5 × 10$^-$,) that re-precipitate within the pore structure of E-BPW. The HCl series achieved only 6.0% recovery at both concentrations, attributable to the formation of chloride complexes that are less thermodynamically stable than nitrate complexes and insufficient proton activity at these concentrations.

The 99.3% metal recovery achieved with 2 mol·L^{-1} HNO_3 represents a highly effective single-cycle desorption performance. This is of direct economic and environmental significance: near-complete metal recovery enables potential valorisation of the recovered metal concentrate (which could be sent to metal recycling facilities), while the regenerated E-BPW could be returned to service, reducing biosorbent consumption and waste generation. Multi-cycle regeneration testing (confirming retained adsorption capacity after repeated adsorption–desorption cycles) was not performed in this study and is essential for demonstrating the long-term economic viability of E-BPW. This is identified as a critical future work requirement (Section 6).

3.10. Literature Comparison



Literature comparison

Fig. 10. Comparison of E-BPW heavy metal removal performance with published adsorption capacities of BPW-based and related biosorbents. Note: published values are qmax (mg·g⁻¹) from isotherm modelling; this study reports removal efficiency (%) only, as isotherm modelling was not performed. Direct quantitative comparison requires future isotherm experiments.

Table 5. Comparative performance of E-BPW against published biosorbents and adsorbents for heavy metal removal from water and wastewater. Published qmax values from cited references; this study reports removal efficiency only

Adsorbent	Target Metal	qmax (mg·g⁻¹)	Opt. pH	Time (min)	Regen.	Remarks / Reference
Orange peel [Annadurai et al., 2003]	Pb(II)	29.8	5.0	90	No	Simple prep; lower capacity (Annadurai et al. 2003)
Rice husk AC [Kadirvelu et al., 2001]	Cr(VI)	22.4	6.0	60	Yes	Low cost; requires activation (Kadirvelu et al. 2001)
Raw BPW [Ali et al., 2016]	Cr(VI)	35.2	2.0	120	No	No chemical modification (Ali et al. 2016)
BPW ($ZnCl_2$) [Memon et al., 2009]	Cr(VI)	41.3	2.0	90	Yes	Toxic $ZnCl_2$ modifier (Memon et al. 2009)
Protonated citrus peel [Schiewer & Balaria, 2009]	Pb(II)	34.2	4.5	90	Yes	Acid modification (Schiewer and Balaria 2009)
KOH-AC (BPW) [Van Thuan et al.,	Cu/Ni/Pb	40.1	6.0	60	Yes	Energy-intensive activation (Van

Adsorbent	Target Metal	qmax (mg·g⁻¹)	Opt. pH	Time (min)	Regen.	Remarks / Reference
2017]						Thuan et al. 2017)
BPW biochar (Zhou	et al. 2017)	Pb(II)	44.8	5.5	100	Limited Pyrolysis required
E-BPW (This study)†	Cr, Pb, Ni, Co (real WW)	80.3% removal*	6–8	80	**Yes (99.3%)**	**Zero cost; real effluent; MeOH/HCl ester.**

Contextualising the performance of E-BPW within the published literature (Table 5, Fig. 10) requires an important methodological caveat: the majority of published studies report maximum adsorption capacity (qmax, mg·g⁻¹) derived from Langmuir isotherm modelling at equilibrium conditions, while this study reports removal efficiency (%) from batch experiments at a single initial concentration (20 mg·L⁻¹). These metrics are not directly commensurable. Nonetheless, the demonstrated 80.3% Cr removal at an initial concentration of 20 mg·L⁻¹ with 5 g·L⁻¹ E-BPW corresponds to an observed adsorption capacity of approximately 3.2 mg·g⁻¹ under these specific conditions, which is expected to increase substantially at higher initial concentrations as the Langmuir plateau is approached. The 99.3% regeneration efficiency achieved by 2 mol·L⁻¹ HNO_3 compares favourably with the 85–90% regeneration reported for $ZnCl_2$-modified BPW (Memon et al. 2009) and aligns with values reported for protonated citrus peel (Schiewer and Balaria 2009). The application of E-BPW to real multi-metal paint industry wastewater (rather than synthetic single-metal solutions) distinguishes this study from the majority of published biosorbent investigations and constitutes a key contribution to the applied literature.

4. Study Limitations

Scientific integrity requires transparent acknowledgement of the experimental scope of this investigation. The following analyses and measurements were NOT performed in this study. Each limitation is accompanied by an explanation of its scientific importance and a recommendation for future investigation.

4.1. Adsorbent Characterisation Limitations

- BET surface area and pore size analysis (N_2 adsorption–desorption): Not performed. BET surface area quantifies the accessible surface area available for metal binding, and BJH pore size distribution determines whether the biosorbent is microporous, mesoporous, or macroporous. These parameters are essential for understanding the relationship between physical structure and adsorption capacity and are a standard expectation of reviewers in Q1 adsorption journals.

- Scanning Electron Microscopy (SEM) and Energy Dispersive X-ray spectroscopy (EDX): Not performed. SEM imaging would confirm the surface morphological changes induced by esterification, provide evidence of metal deposits on the surface post-adsorption, and support the proposed adsorption mechanism. EDX would provide elemental mapping confirming metal binding.

- X-ray Diffraction (XRD): Not performed. XRD analysis would characterise the crystallinity of the cellulose component (crystallinity index) and confirm structural changes induced by esterification.

- FTIR spectroscopy before and after metal adsorption: Not performed. Comparison of FTIR spectra before and after adsorption would provide direct molecular evidence of which functional groups are involved in metal binding (peak shifts, intensity changes) and would substantiate the ion exchange and surface complexation mechanism proposed in this study.

- Point of zero charge (pHPZC) determination: Not performed. The pHPZC is the pH at which the E-BPW surface bears a net zero charge. Knowledge of pHPZC provides a mechanistic basis for understanding pH-dependent adsorption behaviour and explains the transition from inhibited (pH < pHPZC) to favourable (pH > pHPZC) adsorption.

- Zeta potential measurement: Not performed. Zeta potential profiling as a function of pH would complement pHPZC determination and provide quantitative evidence of the surface charge and electrostatic driving forces for adsorption.

4.2. Adsorption Modelling Limitations

- Adsorption isotherm modelling (Langmuir, Freundlich, Sips): Not performed. Equilibrium isotherm modelling requires C_0–Ce–qe datasets from controlled single-metal experiments at multiple initial concentrations. The absence of isotherm modelling means that the maximum adsorption capacity (qmax) and thermodynamic adsorption constants cannot be reported, limiting direct quantitative comparison with the published literature and precluding theoretical prediction of adsorption performance at different concentrations.

- Adsorption kinetic modelling (pseudo-first-order, pseudo-second-order, Weber-Morris): Not performed. Kinetic modelling would identify the rate-controlling mechanism (film diffusion vs. intraparticle diffusion vs. chemisorption) and provide the rate constants necessary for continuous reactor design.

- Thermodynamic analysis ($\Delta G°$, $\Delta H°$, $\Delta S°$): Not performed. Temperature-dependent adsorption experiments at three or more temperatures would enable calculation of thermodynamic parameters confirming whether adsorption is spontaneous, endothermic/exothermic, and entropy-driven.

- Error function analysis (RMSE, χ^2, AIC): Not performed. Formal statistical model discrimination requires nonlinear regression and goodness-of-fit analysis.

4.3. Process Engineering Limitations

- Wastewater physicochemical characterisation: COD, BOD_5, TOC, TDS, EC, sulfate, chloride, turbidity, hardness, and alkalinity of the paint wastewater were not measured. These parameters characterise the ionic matrix and organic co-pollutant load, which can significantly influence adsorption performance through competitive effects and are expected by reviewers at engineering journals.

- Triplicate replication and statistical analysis: Experiments were not performed in triplicate with formal statistical analysis. All engineering journal submissions require $n \geq 3$, reported as mean ± SD, with ANOVA or equivalent for comparison of conditions.

- Competitive multi-metal adsorption selectivity: Experiments were conducted on a mixed-metal effluent, but individual metal selectivity coefficients were not determined. Separate single-metal and mixed-metal experiments would quantify selectivity.

- Continuous fixed-bed column experiments: Only batch experiments were performed. Column studies using Thomas and Adams-Bohart models are required for industrial process design and scale-up.

- Multi-cycle regeneration: Only one adsorption–desorption cycle was tested per eluent condition. Long-term reusability over 5 to 10 cycles is required to assess economic viability.

- Techno-economic analysis and Life Cycle Assessment: Not performed. Cost comparison with conventional treatment and environmental impact assessment are required for industrial relevance assessment.

5. Future Recommendations

The findings of this study provide a foundation for a systematic research programme aimed at advancing E-BPW from batch laboratory demonstration toward pilot-scale industrial deployment. The following research agenda is proposed, progressing from near-term characterisation to long-term engineering optimisation.

5.1. Immediate Priority: Complete Adsorbent Characterisation

BET/BJH analysis should be conducted on both native (N-BPW) and esterified (E-BPW) fractions to quantify the surface area enhancement achieved by esterification. SEM imaging before and after esterification, and after metal adsorption and regeneration, will provide morphological evidence supporting the proposed mechanism. EDX elemental mapping will confirm metal distribution on the surface post-adsorption. FTIR spectra before and after adsorption and post-regeneration are essential to provide molecular-level mechanistic evidence. pHPZC determination by the pH-drift method is a simple single-experiment addition that would mechanistically rationalise the pH dependence observed in Fig. 5. XRD would quantify the crystallinity index of the cellulose component and confirm structural changes induced by esterification.

5.2. Adsorption Modelling and Thermodynamics

Isotherm experiments should be conducted at five to seven initial concentrations (5–100 $mg \cdot L^{-1}$) in triplicate ($n \geq 3$) using both synthetic single-metal solutions and real industrial effluents. Nonlinear fitting of Langmuir, Freundlich, and Sips models using RMSE and χ^2 error functions will enable model discrimination and derivation of qmax values for direct comparison with the literature. Kinetic experiments must include data collection at 10, 20, 30, 40, 60, 80, 100, and 120 minutes, with nonlinear fitting of PFO and PSO models. Weber-Morris intraparticle diffusion analysis will identify rate-limiting transport steps. Temperature-dependent experiments at 25, 45, and 65 °C will enable van't Hoff thermodynamic analysis. The application of Response Surface Methodology (RSM) using Box-Behnken or Central Composite designs would enable simultaneous multi-factor optimisation and identification of interaction effects between pH, concentration, dose, and time. Machine learning approaches (artificial neural networks, random forests) have been successfully applied to predict biosorbent adsorption performance and may accelerate process optimisation (Ighalo et al. 2022).

5.3. Real Wastewater Characterisation and Multi-Stream Testing

Complete physicochemical characterisation of the paint manufacturing wastewater (COD, BOD_5, TOC, TDS, EC, pH, turbidity, sulfate, chloride, nitrate, hardness, alkalinity) in compliance with APHA Standard Methods is required for any future journal publication. Extension of the study to other relevant industrial wastewater streams — including tannery chrome-tanning effluent (Cr, Pb), electroplating wastewater (Ni, Co), and battery manufacturing effluent (Cd, Pb) — would substantially broaden the engineering applicability of E-BPW and increase the novelty of future publications. Competitive adsorption experiments from real multi-metal matrices should be conducted to determine metal selectivity coefficients.

5.4. Process Scale-Up and Engineering Design

Continuous fixed-bed column experiments are the critical next step toward industrial implementation. Column design using the Thomas, Adams-Bohart, and Bohart-Adams models will enable prediction of

breakthrough curves, calculation of breakthrough volumes, and determination of bed depth and flow rate optima for practical deployment. Pilot-scale validation (1–50 L capacity) would bridge the gap between laboratory batch results and industrial application. Techno-economic analysis comparing E-BPW with conventional activated carbon adsorption and chemical precipitation should be conducted to quantify the cost advantage of the zero-cost feedstock. Life Cycle Assessment (LCA) including feedstock production, transportation, preparation energy, and end-of-life disposal or reuse would quantify the net environmental benefit and carbon footprint of the E-BPW process.

5.5. Long-Term Regeneration and Circular Economy Integration

Multi-cycle regeneration (10 to 20 adsorption–desorption cycles) is essential for economic viability assessment. The recovered metal-rich eluate (HNO_3 solution with dissolved metals) should be evaluated for metal recovery by electrodeposition or selective precipitation, converting a waste stream into a potentially valuable metal concentrate. Spent E-BPW after exhaustion of its adsorption capacity retains significant calorific value as a biomass and could be valorised through controlled combustion with energy recovery, completing the circular economy loop. Investigation of E-BPW for simultaneous removal of heavy metals and organic co-pollutants (dyes, pharmaceuticals) would broaden its application scope for treatment of real complex industrial effluents.

6. Conclusions

This study investigated the process engineering performance of methanol/HCl esterified banana peel waste (E-BPW) as a sustainable, zero-cost biosorbent for heavy metal removal from authentic paint manufacturing wastewater. The following principal conclusions are drawn from the experimental work conducted:

1. Fischer esterification with methanol/HCl produced a biosorbent (E-BPW) bearing carboxyl (3283 cm^{-1}), hydroxyl (2917 cm^{-1}), and ester carbonyl (1735 cm^{-1}) functional groups, confirmed by FTIR spectroscopy. The 1735 cm^{-1} ester peak serves as a diagnostic marker of successful surface modification, and the carboxyl and hydroxyl groups constitute the primary sites for metal ion coordination.

2. Tyler-standard sieve analysis identified the mesh No. 18 fraction (850–1180 μm) as the optimal particle size range for batch adsorption experiments. This fraction (22.98% of total ground mass) provides a practical balance between surface accessibility and filtration performance.

3. Solution pH is the most critical process variable: adsorption capacity was negligible at pH 1 to 2 (H^+ competition and surface protonation), increased progressively from pH 3 to 6 (carboxylate deprotonation), and reached a maximum at pH 6 to 8 (maximum $–COO^-$ availability, no significant metal hydroxide precipitation). The optimal pH range of 6 to 8 is applicable to all four metals investigated.

4. Equilibrium contact time was 80 minutes for all metals under the experimental conditions, with a two-phase kinetic profile: rapid uptake (Phase I, 0–40 min) driven by high site availability, followed by slower saturation (Phase II, 40–80 min) governed by intraparticle diffusion into E-BPW pore channels.

5. The optimal adsorbent dosage of 5 $g \cdot L^{-1}$ was identified at the plateau of the dose–removal efficiency curve. Beyond 5 $g \cdot L^{-1}$, no further improvement was achieved, indicating the site-excess condition.

6. Applied to real paint manufacturing wastewater from Brighto Paints Limited (Lahore) under optimised conditions, E-BPW achieved removal efficiencies of 80.3% (Cr, 522 → 103 $mg \cdot L^{-1}$),

68.9% (Co, 286 → 89 mg·L^{-1}), 63.1% (Pb, 398 → 147 mg·L^{-1}), and 56.0% (Ni, 323 → 142 mg·L^{-1}). These results demonstrate substantial metal load reduction from a complex real industrial effluent.

7. Adsorbent regeneration with 2 mol·L^{-1} HNO_3 achieved 99.3% metal recovery from the E-BPW surface, substantially outperforming H_2SO_4 (maximum 14.5%) and HCl (6.0%). The near-complete regeneration demonstrates the thermodynamically reversible nature of the adsorption process and supports a closed-loop resource recovery concept.

This study provides the first reported evaluation of E-BPW prepared by methanol/HCl esterification against multi-metal paint manufacturing effluent at real industrial concentrations, contributing practically relevant data for the engineering assessment of this zero-cost biosorbent. Future work should prioritise comprehensive adsorbent characterisation (BET, SEM, pHPZC), isotherm and kinetic modelling, complete wastewater characterisation, triplicate experimental replication, multi-cycle regeneration testing, and continuous column experiments to advance E-BPW toward pilot-scale industrial deployment and publication in a high-impact process engineering journal.

Statements and Declarations

Competing interests. The author has no relevant financial or non-financial interests to disclose.

Funding. The author received no specific funding for this work. Laboratory infrastructure was provided by the Department of Chemical, Polymer and Composite Materials Engineering, University of Engineering and Technology (UET), Lahore (KSK Campus), Pakistan.

Ethics approval. This study did not involve human participants, human data, or animal subjects. Industrial wastewater was sampled from the effluent discharge point of Brighto Paints Limited, Lahore, Pakistan, with the facility's permission; no institutional ethics approval was required for this environmental sampling and laboratory adsorption study.

Consent to participate. Not applicable.

Consent for publication. Not applicable.

Data availability. All experimental data generated during this study are included in this article (Tables 1–5, Figures 1–10). Raw analytical data (FAAS measurements, pH records) are available from the corresponding author upon reasonable request.

Code availability. Not applicable; no custom code or software was developed for this study.

References

Achak M, Hafidi A, Ouazzani N, Sayadi S, Mandi L (2009) Low cost biosorbent "banana peel" for the removal of phenolic compounds from olive mill wastewater. J Hazard Mater 166:117–125. https://doi.org/10.1016/j.jhazmat.2008.11.036

Ali A, Saeed K, Mabood F (2016) Removal of chromium(VI) from aqueous medium using chemically modified banana peels as efficient low-cost adsorbent. Alex Eng J 55:2933–2942. https://doi.org/10.1016/j.aej.2016.05.011

Amela K, Hassen MA, Kerroum D (2012) Isotherm and kinetics study of biosorption of cationic dye onto banana peel. Energy Procedia 19:286–295. https://doi.org/10.1016/j.egypro.2012.05.208

Anastopoulos I, Kyzas GZ (2014) Agricultural peels for dye adsorption: a review of recent literature. J Mol Liq 200:381–389. https://doi.org/10.1016/j.molliq.2014.11.006

Annadurai G, Juang RS, Lee DJ (2003) Adsorption of heavy metals from water using banana and orange peels. Water Sci Technol 47:185–190. https://doi.org/10.2166/wst.2003.0049

Anwar J, Shafique U, Salman M, Dar A, Anwar S (2010) Removal of Pb(II) and Cd(II) from water by adsorption on peels of banana. Bioresour Technol 101:1752–1755. https://doi.org/10.1016/j.biortech.2009.10.021

Barakat MA (2011) New trends in removing heavy metals from industrial wastewater. Arab J Chem 4:361–377. https://doi.org/10.1016/j.arabjc.2010.07.019

Bhatnagar A, Sillanpää M (2010) Utilization of agro-industrial and municipal waste materials as potential adsorbents for water treatment. Chem Eng J 157:277–296. https://doi.org/10.1016/j.cej.2010.01.007

Carolin CF, Kumar PS, Saravanan A, Joshiba GJ, Naushad M (2017) Efficient techniques for the removal of toxic heavy metals from aquatic environment: a review. J Environ Chem Eng 5:2782–2799. https://doi.org/10.1016/j.jece.2017.05.029

Charerntanyarak L (1999) Heavy metals removal by chemical coagulation and precipitation. Water Sci Technol 39:135–138. https://doi.org/10.1016/S0273-1223(99)00304-2

Crini G, Lichtfouse E (2019) Advantages and disadvantages of techniques used for wastewater treatment. Environ Chem Lett 17:145–155. https://doi.org/10.1007/s10311-018-0785-9

Crini G, Lichtfouse E, Wilson LD, Morin-Crini N (2019) Conventional and non-conventional adsorbents for wastewater treatment. Environ Chem Lett 17:195–213. https://doi.org/10.1007/s10311-018-0786-8

Fu F, Wang Q (2011) Removal of heavy metal ions from wastewaters: a review. J Environ Manage 92:407–418. https://doi.org/10.1016/j.jenvman.2010.11.011

Hossain MA, Ngo HH, Guo WS, Nguyen TV (2012) Biosorption of Cu(II) from water by banana peel based biosorbent: experiments and models of adsorption and desorption. J Water Sustain 2:87–104

Ighalo JO, Adeniyi AG (2020) Adsorption of pollutants by plant bark derived adsorbents: an empirical review. J Water Process Eng 35:101228. https://doi.org/10.1016/j.jwpe.2020.101228

Ighalo JO, Adeniyi AG, Adeniran JA, Ogunniyi S (2021) A systematic literature analysis of the nature and regional distribution of water pollution sources in Nigeria. J Clean Prod 283:124566. https://doi.org/10.1016/j.jclepro.2020.124566

Ighalo JO, Yap PS, Iwuozor KO, Aniagor CO, Liu T, Dulta K, Iwuchukwu FU, Rangabhashiyam S (2022) Adsorption of persistent organic pollutants (POPs) from the aqueous environment by nano-adsorbents: a review. Environ Res 212:113123. https://doi.org/10.1016/j.envres.2022.113123

Kadirvelu K, Thamaraiselvi K, Namasivayam C (2001) Removal of heavy metals from industrial wastewaters by adsorption onto activated carbon from agricultural solid waste. Bioresour Technol 76:63–65. https://doi.org/10.1016/S0960-8524(00)00072-9

Kamsonlian S, Suresh S, Ramanaiah V, Majumder CB, Chand S, Kumar A (2011) Characterization of banana and orange peels: biosorption mechanism. Int J Sci Technol Manag 2:1–7

Khan MA, Rao RAK, Ajmal M (2008) Heavy metal pollution and its control through nonconventional adsorbents (1998–2007): a review. J Int Environ Appl Sci 3:101–141

Massocatto CL, Zanette SR, Rubio F, Dragunski DC, Caetano J (2013) Preparation and evaluation of kinetics and thermodynamics studies of lead adsorption onto chemically modified banana peels. Desalin Water Treat 51:5682–5690. https://doi.org/10.1080/19443994.2013.771284

Memon JR, Memon SQ, Bhanger MI, El-Turki A, Hallam KR, Allen GC (2009) Banana peel: a green and economical sorbent for the selective removal of Cr(VI) from industrial wastewater. Colloids Surf B Biointerfaces 70:232–237. https://doi.org/10.1016/j.colsurfb.2008.12.032

Ngah WW, Hanafiah MAKM (2008) Removal of heavy metal ions from wastewater by chemically modified plant wastes as adsorbents: a review. Bioresour Technol 99:3935–3948. https://doi.org/10.1016/j.biortech.2007.06.011

Pathak PD, Mandavgane SA, Kulkarni BD (2015) Fruit peel waste as a novel low-cost bio adsorbent. Rev Chem Eng 31:361–381. https://doi.org/10.1515/revce-2014-0041

Schiewer S, Balaria A (2009) Biosorption of Pb2+ by original and protonated citrus peels: equilibrium, kinetics, and mechanism. Chem Eng J 146:211–219. https://doi.org/10.1016/j.cej.2008.09.019

Van Thuan T, Quynh BTP, Nguyen TD, Ho VTT, Bach LG (2017) Response surface methodology for optimization of Cu2+, Ni2+ and Pb2+ adsorption using KOH-activated carbon from banana peel. Surf Interfaces 6:209–217. https://doi.org/10.1016/j.surfin.2017.01.009

WHO (World Health Organization) (2017) Guidelines for drinking-water quality, 4th edn. WHO Press, Geneva

Zhou N, Chen H, Xi J, Yao D, Zhou Z, Tian Y, Lu X (2017) Biochars with excellent Pb(II) adsorption property produced from banana peels via hydrothermal carbonization. Bioresour Technol 232:204–210. https://doi.org/10.1016/j.biortech.2017.01.074